The unusual nanostructure of nickel–boron catalyst†

Junfeng Geng,* David A. Jefferson and Brian F. G. Johnson*

Received (in Cambridge, UK) 26th October 2006, Accepted 27th November 2006
First published as an Advance Article on the web 11th December 2006
DOI: 10.1039/b615529d

A highly unusual nanostructure of the nickel–boron particulate material, initially synthesised in the 1950s and well known to be an exceedingly active hydrogenation catalyst, has been identified for the first time.

In 1953 Shlesinger and co-workors reported that the reduction of a nickel salt with sodium borohydride in aqueous solution yields a finely divided black material as a precipitate that contains both nickel and boron.[1] This material was further shown to have extraordinary catalytic activity for a wide variety of hydrogenation reactions.[2–5] These findings triggered subsequent extensive studies by recognizing the significance and complexity of this catalyst, focused primarily on its stoichiometric chemistry,[6–8] chemical state of the surface[9–11] and the catalytic applications.[12–15] However, the structure of the material has remained unclear for over 50 years. Studies so far by using powder X-ray diffraction (XRD),[10,16,17] X-ray photoelectron spectroscopy (XPS)[9,11,18,19] and transmission electron microscopy (TEM),[12,16*b*,17,19] have led to a view that this material is amorphous, and as a consequence it is frequently called an "amorphous alloy". Here we report that, instead of being amorphous, the material possesses a highly unusual nanostructure. We find that this material is composed of nickel–boron nanoparticles in which very small nickel single crystals form clusters as host that holds guest boron species captive within their interstitial sites.

The synthesis of the material was carried out by following the original route using nickel acetate ($Ni(CH_3COO)_2{\cdot}4H_2O$) and sodium borohydride ($NaBH_4$).[1–4] Examination of the material by TEM showed that it consists of nanoparticles within the size range of 10–30 nm (Fig. 1(a)). Detailed observations using high-resolution TEM revealed that these nanoparticles are not amorphous but possess an ultra-fine crystalline structure (Fig. 1(b), (c)). Each particle is composed of a number of smaller component particles with a size of 1–3 nm. These tiny components, although extremely small, with the smallest showing only five lattice fringes, are nevertheless clearly crystalline. They are tightly clustered together, giving each complete particle a clear boundary from its neighbours. The resulting structure is in marked contrast to that of conventional colloidal nickel nanoparticles which are usually well-defined single crystals. Within the networks of gaps formed between these crystalline components, and around the complete ensemble, a second amorphous phase was observed, which we believe prevents the sintering of the small crystals.

Department of Chemistry, University of Cambridge, Cambridge, UK CB2 1EW. E-mail: bjohnson@freenet.co.uk; jg201@cam.ac.uk; Fax: +44 (0)1223 336362; Tel: +44 (0)1223 336335

† Electronic supplementary information (ESI) available: Experimental details for the synthesis and characterisation of the material. See DOI: 10.1039/b615529d

Previous studies using XPS have found that the binding energy of Ni $2p_{3/2}$ in this material is consistent with that of the bulk nickel (~852.5 eV),[9,11,19] suggesting the elemental state of the metal. However, regarding the boron involved, two forms have been observed which correspond to the binding energy of B 1s at 188.2 and 191.7 eV, respectively. These two forms were assigned to the elemental B associated with nickel and the B in the deposited BO_2^- ions resulting from the hydrolysis of $NaBH_4$.[9] In similar materials and from the systems of Pd–B and Pt–B, the third form of boron with characteristic low binding energies around 182 eV, which is believed to arise from a hydrogen-containing boron (denoted as B–H), has also been observed.[6,9] Considering these findings, we expect that in our sample, the observed component crystallites are of metallic nickel, and the captive surface phase is due to boron-containing species.

In order to test this hypothesis, we first imaged many nanoparticles at random to avoid any long-time exposure to the electron beam. These observations yielded consistent results and all particles were found to possess the same nanostructure. Nano-beam electron diffraction was carried out over selected areas of the

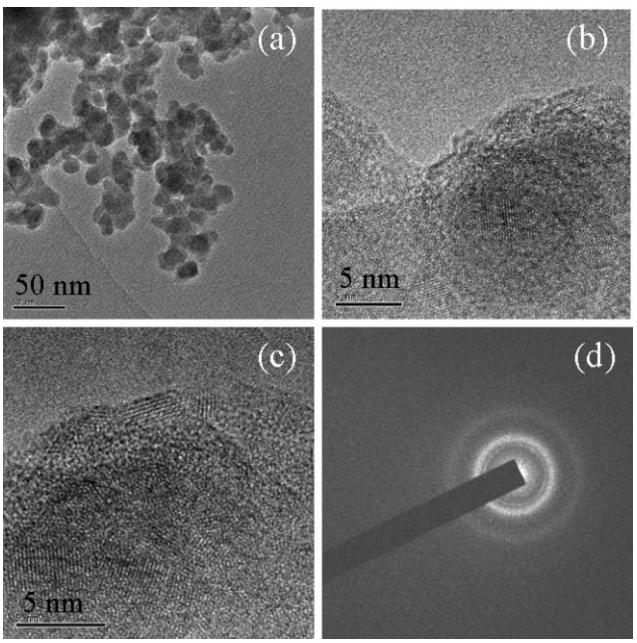

Fig. 1 TEM images of the nickel–boron nanoparticles as precipitate of the reaction of $Ni(CH_3COO)_2$ with $NaBH_4$ in aqueous solution. (a) A low-magnification image shows the size and morphology of the nanoparticles. (b) A higher magnification (×600 000) image of a typical particle in the precipitate; (c) The image (b) at a higher resolution (×800 000) shows the lattice fringes of the tiny nickel crystallites as component in different orientations; (d) The nano-beam electron diffraction rings of the sample.

sample. Only particles which protruded over holes of the carbon/plastic support film were studied in order to eliminate any contribution of amorphous carbon to the diffraction rings. Diffraction patterns showed three rings only, which are the inner relatively sharp ring, a much stronger but more diffuse middle ring and a diffuse outer ring (Fig. 1(d)). These gave the *d* spacing of the corresponding lattices: inner, 2.506 Å; middle, 2.094 Å and outer, 1.231 Å. The strong middle ring could correspond to either (111) of Ni or (200) of NiO, and the outer ring to (220) Ni or (311) NiO. The inner sharp ring did not fit with any known line of these phases, but it matched exactly to the forbidden (110) spacing of metallic nickel. Given the extremely small size of the particles, it is highly possible that the normal systematic absence conditions break down and this diffraction is consequently allowed. Moreover, the absence of the strong (111) and (220) lines of nickel oxide in the diffraction patterns suggests that the component crystals would not be oxide but metallic nickel.

Powder XRD studies on both the as-prepared and then thermally annealed sample were also performed. The results are shown in Fig. 2. As expected, the raw material shows a complete absence of any sharp diffraction peaks, and only a broad diffraction peak at around $2\theta = 45^\circ$ appears, consistent with the literature reports.[10,16,17] Moreover, previous studies assigned this broad peak to be associated with amorphous nickel. But here, our HRTEM observation of the ultra-fine crystalline structure clearly indicates that although the component particles are extremely small they are well crystalline. Almost certainly, this broad X-ray diffraction peak arises from these extremely small crystalline component particles. This peak probably corresponds to the (111) reflection of Ni (d = 2.02–2.04 Å).[20] Thermal treatment of the sample at 600 °C in argon dramatically improved the quality of the XRD profile because of the increased crystallization by sintering of the small crystals. The three strongest diffraction lines of metallic nickel were then fully developed (Fig. 2(b)), consistent with the literature report.[17] They correspond to the peaks at 2θ = 44.45, 51.73 and 76.84°, and match exactly to the Ni(111), Ni(200) and Ni(220) reflections, respectively.[20]‡ This result was subsequently confirmed by the HRTEM examination of the annealed sample where larger metallic Ni nanoparticles were clearly observed. On

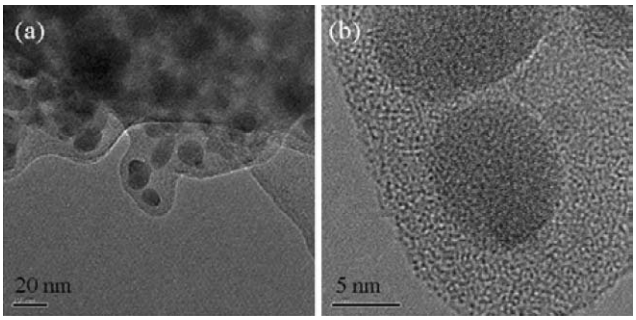

Fig. 3 Low-magnification (a) and high-magnification (b) TEM images of the nickel–boron nanoparticles prepared with an excess of boron, to show the amorphous boron coating on the particle surface. In this case, the molar ratio of the nickel acetate to sodium borohydride was 1 : 3.

the basis of these findings, coupled with the electron diffractions as well as the previous XPS results, we conclude that the component crystals in our sample are of metallic nickel.

HRTEM observations also revealed an amorphous coating on most of the nanoparticles, and that some crystallization of this coating could be induced upon prolonged exposure to the electron beam. Repetition of the reaction under the same conditions but using higher content of the borohydride led to a much thicker coating as shown in Fig. 3. Moreover, the metallic structure of the particles remained unchanged with the increase in boron content. Faint, superimposed fringes could still be discerned in the cores of the particles.

X-Ray emission energy dispersive spectroscopy (EDS) measurements were performed on the specimens with the differing boron contents. As boron is difficult to detect due to its low emission energy (~188 eV), a preliminary investigation was carried out on B_2O_3 to ascertain detection limits. To avoid reduction in the electron beam, this preliminary study utilized large diameter beams (1–10 μm) and spectra were recorded from the same area after different irradiation times to test for consistency. Under these conditions, no sample reduction was observed. The observed boron K-emission peak is shown in Fig. 4. For the original

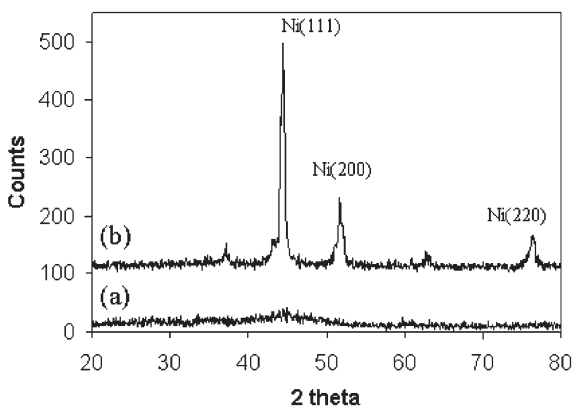

Fig. 2 Powder XRD diffraction profiles of the as-prepared nickel–boron nanoparticles (a), and then thermally annealed sample at 600 °C in an argon atmosphere (b). The assigned diffraction peaks in (b), from left to right, correspond to the *d* spacing of 2.03, 1.73 and 1.25 Å, respectively, for metallic nickel.

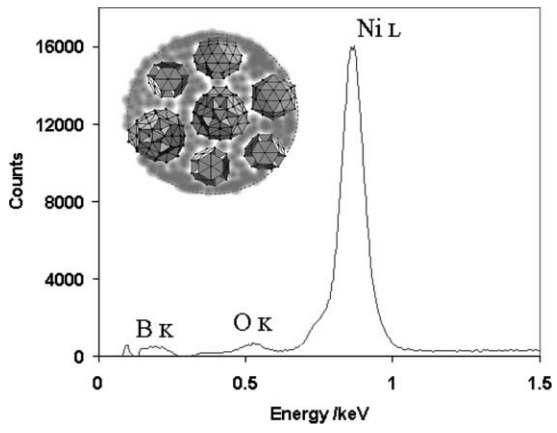

Fig. 4 EDS analytical result shows the elements present in the material and their corresponding X-ray emission peaks. Inset: a schematic diagram shows the fine structure of the nickel–boron nanoparticles. It is made up of a cluster of tiny nickel single crystallites (1–3 nm) as host that appears to hold a boron-containing species captive in their interstitial spaces.

specimen prepared with the reactants molar ratio of 1 : 1, multiple EDS analyses gave a mean O(K-edge)/B(K-edge) peak intensity ratio of 1.13. Some areas showed almost no oxygen at all in the specimen. The specimen precipitated with an excess of $NaBH_4$ (the molar ratio of the acetate to the borohydride was 1 : 3) showed a even smaller O(K-edge)/B(K-edge) ratio at $\sim$0.84, implying a greater boron content, consistent with the HRTEM observation for the greater thickness of the amorphous coating. These data may be compared with the measured much larger oxygen content in B_2O_3, with the O(K-edge)/B(K-edge) ratio found to be 13.87, indicating that the boron present in the sample was not oxide. This, coupled with the large difference in image contrast between the coatings and the particle cores, confirms that the coating was a boron-containing species, probably a pure boron in an amorphous form. A schematic diagram relating to the structure of these nickel boron nanoparticles is shown as an inset of Fig. 4.

In summary, this work provides the first HRTEM observation of the ultra-fine structure of the nickel catalyst. Unlike the earlier suggestion that this material is amorphous, our studies reveal that it is not amorphous but actually possesses a highly unusual nanostructure which is made up of tiny nickel crystallites (1–3 nm) bound in the matrix of boron-containing species. Almost certainly, the boron acts to "cement" the crystallites together and prevents their subsequent sintering. This interesting combination of the two elements allows the nickel particles to remain extremely small in size with a consequent very high surface area, offering an explanation why the catalyst is exceedingly active for a wide range of hydrogenation reactions. In addition, as the studies of this Ni–B system have been widely extended to the chemical reduction of other transition metals including Fe, Co, Ni, Cr, Mn, Mg, Pd and Cu by borohydride,[7–19] our findings open up a new avenue to the understanding of the fascinating nanostructures of similar metal–boron alloys.

We are grateful for financial support from the EU EXCELL project. The JEM-3011 electron microscope and PGT Avalon 2000 EDS system were funded by EPSRC grant M51109.

Notes and references

‡ Three other weak diffraction peaks in the XRD spectrum, with d = 2.09, 2.41 and 1.48 Å, respectively, correspond to NiO.[21] This was further confirmed by the EDS measurements coupled with their high-resolution TEM images. EDS analyses of the original specimens showed no such NiO phase. Consequently this oxide was believed to result from the reaction of the component Ni crystals with the sample-contained H_2O in the heating process, to first form $Ni(OH)_2$ which subsequently decomposed into NiO

1 H. I. Schlesinger, H. C. Brown, A. E. Finholt, J. R. Gilbreath, H. R. Hoekstra and E. K. Hyde, *J. Am. Chem. Soc.*, 1953, **75**, 215.
2 H. C. Brown and C. A. Brown, *J. Am. Chem. Soc.*, 1962, **84**, 1493.
3 H. C. Brown, C. A. Brown and H. C. Brown, *J. Am. Chem. Soc.*, 1963, **85**, 1003.
4 C. A. Brown, *J. Org. Chem.*, 1970, **35**, 1900.
5 C. A. Brown and V. K. Ahuja, *J. Org. Chem.*, 1973, **38**, 2226.
6 P. C. Maybury, R. W. Michell and M. F. Hawthorne, *J. Chem. Soc., Chem. Commun.*, 1974, 534.
7 Y. Chen, *Catal. Today*, 1998, **44**, 3.
8 H. Li, H. Li, W. Dai and M. Qiao, *Appl. Catal., A*, 2003, **238**, 119.
9 Y. Okamoto, Y. Nitta, T. Imanaka and S. Teranishi, *J. Chem. Soc., Faraday Trans. 1*, 1979, **75**, 2027.
10 J. V. Wonterghem, S. Morup, C. J. W. Koch, S. W. Charles and S. Wells, *Nature*, 1986, **322**, 622.
11 J. A. Schreifels, P. C. Maybury and W. E. Swartz, Jr., *J. Catal.*, 1980, **65**, 195.
12 R. C. Wade, D. G. Holah, A. N. Hughes and B. C. Hui, *Catal. Rev. Sci. Eng.*, 1976, **14**, 211.
13 D. G. Holah, I. M. Hoodless, A. N. Hughes and L. Sedor, *J. Catal.*, 1979, **60**, 148.
14 Y. C. Liu, C. Y. Huang and Y. W. Chen, *Ind. Eng. Chem. Res.*, 2006, **45**, 62.
15 H. Li, H. Luo, L. Zhuang, W. Dai and M. Qiao, *J. Mol. Catal. A: Chem.*, 2003, **203**, 267.
16 (*a*) J. E. Hofer, J. F. Shultz, R. D. Panson and R. B. Anderson, *Inorg. Chem.*, 1964, **3**, 1783; (*b*) J. Deng, J. Yang, S. Sheng, H. Chen and G. Xiong, *J. Catal.*, 1994, **150**, 434.
17 Y. He, M. Qiao, H. Hu, Y. Pei, H. Li, J. Deng and K. Fan, *Mater. Lett.*, 2002, **56**, 952.
18 Y. Okamoto, Y. Nitta, T. Imanaka and S. Teranishi, *J. Chem. Soc., Faraday Trans. 1*, 1980, **76**, 998.
19 J. Shen, Z. Hu, Q. Zhang, L. Zhang and Y. Chen, *J. Appl. Phys.*, 1992, **71**, 5217.
20 The International Centre for Powder Diffraction Data, *Powder Diffraction Files*, 2001, Card Numbers: 87-0712; 45-1027; 04-0850; 03-1051; 03-1043; 01-1258.
21 The International Centre for Powder Diffraction Data, *Powder Diffraction Files*, 2001, Card Numbers: 47-1049; 44-1159, 22-1189.